A Dexterous Part-Holding Model for Handling Compliant Sheet Metal Parts

H. F. Li
General Motors Corp,
Warren, MI 48089

D. Ceglarek*
Department of Industrial Engineering,
The University of Wisconsin-Madison,
Madison, WI 53706
e-mail: darek@engr.wisc.edu

Jianjun Shi
Department of Industrial and Operations Engineering,
The University of Michigan-Ann Arbor,
Ann Arbor, MI 48109

Material handling of compliant sheet metal parts significantly impacts both part dimensional quality and production rate in the stamping industry. This paper advances previously developed material handling end effector layout optimization methodology for rigid point end effectors [1] by developing a dexterous part-holding end effector model. This model overcomes the shortcomings of the rigid point part-holding end effector model by predicting part deformation more accurately for various modes of deformation and for a set of part-holding end effector locations. This is especially important for handling systems which utilize vacuum cup end effectors widely used for handling of large sheet metal parts. The dexterous end effector model design method and an algorithm for estimation of model parameters are developed. The algorithm combines data from design of computer simulations and from the set of experiments by integrating finite element analysis and a statistical data processing technique. Experimental studies are conducted to verify the developed model and the model parameter estimation algorithm. The developed methodology provides an analytical tool for product and process designers to accurately predict part deformation during handling, which further leads to minimization of part deformation, improvement of part dimensional quality and increase of production rate.
[DOI: 10.1115/1.1406953]

1 Introduction

Compliant sheet metal parts are widely used in automotive, aerospace, aircraft, appliance, and furniture industries. Material handling of compliant parts poses much greater challenge than the handling of rigid parts since the compliant parts can deform during the handling process. Figure 1 shows an example of a material handling system for compliant parts used in a production stamping line. After a sheet metal part is stamped in one press station, it is picked up and transferred forward to the next press station by the material handling system. In general, large, flat sheet metal parts deform when they are transferred from one press station to the next. The magnitude of part deformation depends on a number of part and process design parameters such as: part compliance, material handling transfer speed, and end effector layout. The deformation of parts strongly impacts part dimensional quality and productivity. The impact of material handling on part quality can be described on two levels:

1 Direct impact—through permanent part deformation occurring during the handling process;
2 Indirect impact—through part elastic deformation occurring during the handling process.

Permanent deformation results in damaging a part and thus is not allowed in design of the material handling process. Based on extensive studies conducted previously [1–3], part elastic deformation during the handling process also has a significant impact on both part dimensional variation and rate of production. Material handling has been identified as one of the top five reasons for part dimensional variation in the automotive industry [1–3]. One of the intrinsic reasons is part elastic deformation occurring during part handling operations.

Part elastic deformation during material handling affects part/subassembly dimensional quality in the following ways:

(a) Part nesting error—error of positioning/dropping parts into the die (installed in the stamping press). Part elastic deformations may cause part positional variation in a die, which can further cause mis-stamping of parts in each press/die (a stamping line for large automotive parts usually has 4–5 presses/dies). These small deviations of the part in each die accumulate and can eventually cause very large dimensional variation of the final part or even produce scrap and/or cause line downtime. For automotive closure panels this large accumulative part variation can be on the level of 4–6 mm or even larger (as measured by 6-sigma)

(b) Part distortion during die contact—parts are usually dropped into the die at the end of the material handling process. If excessive elastic deformations occurs, the contact force between part and die can be so unevenly distributed that the part can be permanently damaged.

(c) Part-obstacle interference—part elastic deformation during transfer increases uncertainty in planning a part transfer trajectory. This may, in effect, cause unexpected interference of the part with the surrounding environment and therefore, damage the part. And it can even cause reduction of production rate to avoid potential interferences.

The lack of ability to accurately predict part elastic deformation during the material handing process can cause design intended dimensional quality of parts unachievable during production. Additionally, the part transfer path may not be the optimal one, and the handling time between stations may not be the shortest thus, resulting in reducing the overall rate of production. Therefore, prediction of part elastic deformation is one of the most critical issues in the material handling of compliant sheet metal parts. In this paper, all considered part deformations are assumed to be elastic.

In some sense, the prediction of part deformation during handling with a given end effector layout is similar to the prediction of workpiece deformation during fixture design process. Fixture modeling and design has been thoroughly studied and significant results have been achieved [4]. Based on the part characteristics the research in fixture design can be categorized into two groups: fixturing of rigid parts and fixturing of compliant parts. For rigid

*Corresponding author.
Contributed by the Manufacturing Engineering Division for publication in the JOURNAL OF MANUFACTURING SCIENCE AND ENGINEERING. Manuscript received June 2000; revised March 2001. Associate Editor: E. C. DeMeter.

Copyright © 2002 by ASME

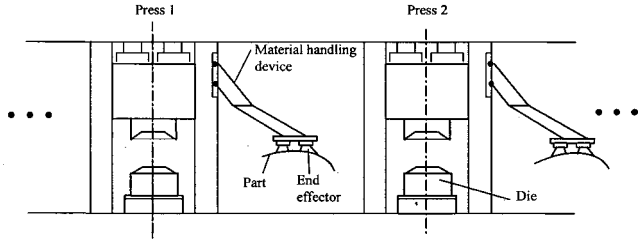

Fig. 1 An example of a material handling system in a stamping line

parts, the functional configuration of fixture is often based on kinematic and mechanical methods such as screw theory [5,6] and force equilibrium equations [7]. In his research on constructing force-closure grasps based on the shape of the grasped object Nguyen [8] classified the locators as frictionless point contact, hard-finger contact and soft-finger contact. DeMeter [9] expanded the fixture design research by considering the planar, spherical and cylindrical surface contacts between the workpiece and fixture elements. Different approaches have also been developed for fixture design optimization [10–12].

Much less research has been done on fixturing for compliant parts. Lee and Haynes [13] proposed a finite element model of the fixturing system analysis for prismatic parts. This research considered workpiece deformation and stresses as well as the friction between the fixture element and the workpiece. Based on this finite element analysis model, many approaches to the optimal fixture design for compliant sheet metal parts have been developed [14–17]. Most recently, Ceglarek et al. [1] extended the traditional fixture design scenario to the material handling of sheet metal parts by adding movability conditions. Although their end effector layout optimization methodology can significantly reduce part deformation during the handling process, the end effectors were modeled as rigid points. This can be applied to material handling systems that use shovels or fingers as end effectors.

However, a significant number of material handling systems use vacuum cup type of end effectors to handle large stamped sheet metal parts. The vacuum cups have some translational and torsional motion flexibility in 3-D space relative to the part handled. The rigid point model does not represent these characteristics and thus cannot predict part deformation accurately. Furthermore, with rigid models, the prediction accuracy of part deformation is not consistent in the whole domain of end effector holding positions/layouts. For some end effector layouts, the rigid model is even unable to estimate part deformation mode correctly (see Fig. 15 in Section 4.4 for more details).

While there are a number of techniques for modeling contact region deformation [18,19], in general, these consider the effect of static loadings on quasi-static workpiece deflection. They assume a workpiece to be an elastic body in frictional contact with rigid elements. This assumed condition is very different from the working conditions of material handling of sheet metal parts, which have been described by Ceglarek et al. [1]. Yeh and Liou [20] proposed a modeling technique to monitor the contact conditions based on dynamic response frequencies of a fixture system. The virtual spring element based on the Hertz theory was used to recapitulate fixture contact conditions in finite element modeling. This research cannot be applied in material handling since the contact stiffness in this research is estimated through force-deformation ratio at contact point, which is invalid in material handling for compliant sheet metal parts as vacuum cups cannot be represented by parallel linear springs.

All the above mentioned research has significantly advanced fixture design for sheet metal parts and is helpful for part deformation control during the material handling process. However, the lack of a dexterous model of end effectors has imposed a constraint on precise part deformation prediction, and further limited the improvement of part dimensional quality and production rate caused by material handling.

This paper attempts to resolve the aforementioned challenges by developing a dexterous part-holding model which models the vacuum cup type of end effectors as several linear springs configured in a 3-D space. By the term ''dexterous,'' we mean that the model incorporates flexibility necessary to reflect the real characteristics of the industrial end effectors. This dexterous model differs from dexterous hand study in robotic research, where the robot hand has many degrees of freedom and each finger and joint can be individually and independently driven [21]. In this paper, the presented research is focused on developing an accurate part-holding model to precisely describe the characteristics of a given vacuum cup-type of end effector, and therefore, to precisely predict part deformation during the material handling process.

In order to develop such a model, first, the structure of the dexterous part-holding end effector model needs to be designed. Second, values for some of the critical but unknown parameters, such as cup stiffness and effective diameter, need to be estimated based on the handling motion direction and velocity profile, part weight and other handling factors. The accurate estimation of dexterous model parameters is critical for the development of the model.

This paper is organized as follows: Section 2 presents the structure design of the dexterous part-holding model. Section 3 presents the methodology for the dexterous model parameter estimation. The developed methodology is then validated through a case study and experiments, which are presented in Section 4. Finally, Section 5 presents summary and conclusions.

2 The Dexterous Model Structure Design

The methodology for development of dexterous part-holding end effector model includes the dexterous model structure design and the model parameter estimation. In this section, we present how to build a dexterous model geometry for a given cup diameter and cup height.

There are two kinds of part-holding end effectors commonly used in the handling of sheet metal parts in a stamping line: vacuum cups and fingers or shovels. Fingers or shovels are usually used to transfer small and rigid parts. Vacuum cups are usually used to transfer large and flat sheet metal parts. In general, there are three types of commonly used vacuum suction cups: round, round convoluted, and oval cups, as shown in Fig. 2.

This paper develops a model for the round vacuum cups. The developed methodology can be easily expanded to model the convoluted and oval cups. The key parameters for the round vacuum cups are: (1) cup material, (2) cup diameter, and (3) cup height. One of the characteristics of the round vacuum cups is that one end, near the holding socket (cup-to-frame joint), is fixed without any degree of freedom to move; the other end, near the handled part (cup-to-part joint), can move along with the part due to the elasticity of the end effector material (Figs. 2 and 3). This characteristic can be represented by a system of springs, which this paper calls a *dexterous part-holding end effector model.*

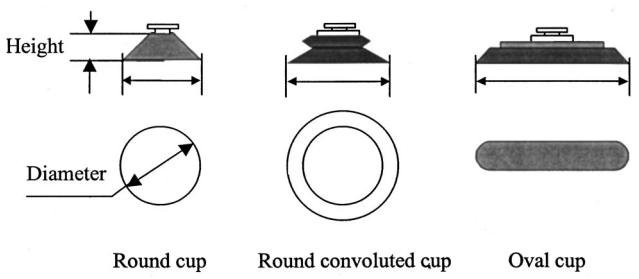

Fig. 2 Commonly used vacuum cups

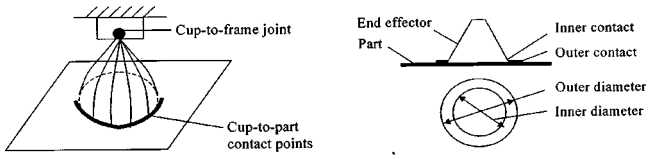

Fig. 3 The cup partly adheres to the part

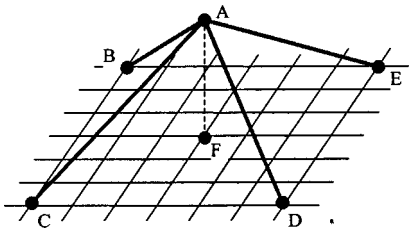

Fig. 4 An example of a dexterous part-holding model

The structure design of the dexterous model is based on two steps:

1 Defining cup-to-frame and cup-to-part joints. The cup-to-frame joint is usually designed as a rigid point. It is simulated in the same manner as in the dexterous model (Fig. 3). The cup-to-part contact region, for round cups, is a ring with large and small diameters, which are determined based on the cup's initial diameter and the dynamic parameters (vacuum level, part weight, etc.). It is simulated as a circle. The diameter of the circle will be determined by the approach presented in Section 3.

2 Discretizing the simulated cup-to-part joints. The circle representing the cup-to-part joints is discretized into a series of points. By connecting these points with the simulated cup-to-frame joint with linear springs, we can obtain a dexterous model (Fig. 3).

The slippage of the handled part relative to cups is not allowed during the transfer process. Otherwise the part may be damaged during handling as discussed in Section 1. Thus, the cup and the handled part are in contact without any slippage at all times during a successful material handling process. Therefore, the static friction in the cup-to-part contact region is reflected through the reaction forces on the node.

Due to the geometric complexity of the sheet metal parts and the part-holding end effectors, Finite Element Analysis (FEA) is used for modeling and simulation, specifically, ABAQUS software. In ABAQUS, each spring in the dexterous model is treated as a spring element. Figure 4 shows an example of the dexterous model consisting of four springs. Point A represents the cup-to-frame joint. Points B, C, D, and E represent discretized cup-to-part contact points. Line segment AB, AC, AD, and AE represent the four springs. Point F is the orthogonal projection of point A into the part plane.

Generally, in the dexterous model of vacuum cups, it is likely that the cup diameter represented by points B through E does not coincide with the FEA nodes. Thus, three approaches can be used

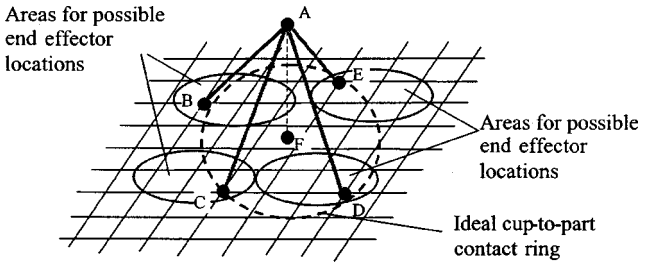

Fig. 5 Approximating the cup size in the spring model

in order for the FEA model to run: (a) to employ shape functions for the finite element, (b) to locally remesh the handled part, or (c) to approximate the cup diameter in the spring model. Employing shape functions can guarantee an exact size of the spring model; however, it needs more effort in generating the model. Locally remeshing can generate a uniform spring model wherever the end effector is located, but more efforts are required in the remeshing process. On the other hand, the approximation of the cup size in the spring model avoids the efforts of employing shape functions and remeshing, though the accuracy depends on the mesh resolution and may be reduced in some cases. Figure 5 illustrates the approximation approach.

In Fig. 5, four areas represent the possible regions that each of the cup-to-part contact points could be located. The regions are determined by the spring model structure design such as the number of springs and their orientations. Within each region, the node, which has the shortest distance to the ideal cup-to-part contact circle, is selected to be the cup-to-part contact point. Therefore, different springs may have different lengths and form different angles to the cup-to-part contact plane in the spring model. For example, spring lengths of AB and AE in Fig. 5 are different.

It can be seen that in the approximation approach, the accuracy of the spring model depends on the mesh density of the part. A finer mesh can lead to a more accurate spring model. This is due to the fact that when the mesh size is smaller, each end effector model will cover a higher number of finite elements. Part deformation caused by changing the end of the spring from inside of the mesh element to the node of this element is of less importance. Therefore, it is acceptable to use the closest node of the mesh element as a position for location of the end of the spring in the proposed model. It can be observed that sensitivity of such approximation varies with the end effector layout changes.

3 Dexterous Model Parameter Estimation

After designing the structure of a dexterous end effector model, the key parameters of the model need to be selected and determined. This section presents the procedure to estimate the key parameters of the model. The key parameters in the dexterous model are stiffness, diameter, and height. Table 1 lists the part-holding end effector types and key parameters for the end effector and for the dexterous model.

The key cup parameters (KCP) cannot be used directly as key model parameters (KMP) in the dexterous model for two main reasons. First, the end effector stiffness is difficult to test. We can only test the equivalent

Table 1 Summary of end effector types and the key parameters

End effector types	Vacuum cup types	Key cup parameters (KCP)	Key model parameters (KMP)
Vacuum cups Fingers or shovels	Round Round convoluted Oval	(1) Stiffness k_c (2) Diameter d_c (3) Height h_c	(1) Stiffness k_m (2) Diameter d_m (3) Height h_m

stiffness of the cup in the direction of its axis by recording the loading and the cup extension or contraction. However, how the cup stiffness can be decomposed in the spring model is not straightforward. Second, the developed dexterous model and the real cup are only functionally equivalent. The dexterous model parameters do not physically map those of the real cup. This can be explained by analyzing the stress conditions inside the cup material. For example, in the static holding, as shown in Fig. 3, the end effector partly adheres to the part surface. Since inside the cup is a vacuum, the cup is in a compressed state. In the spring model, however, the spring undergoes tension and is in an elongated state. Therefore, the measured stiffness of the cup cannot be used as the stiffness of the spring. Additionally, during transfer motion the cup-to-part contact area may vary during different transfer processes and depends on the vacuum pressure level and handling dynamic loading conditions. This means that the effective end effector diameter will change as well. Therefore, the initial cup diameter cannot be taken as the effective diameter for the model.

The goal of the dexterous model parameter estimation is to determine the following relations:

$$\begin{aligned} k_m &= f_1(k_c, d_c, h_c) + \varepsilon_1 \\ d_m &= f_2(k_c, d_c, h_c) + \varepsilon_2 \\ h_m &= f_3(k_c, d_c, h_c) + \varepsilon_3 \end{aligned} \tag{1}$$

where ε_1, ε_2 and ε_3 are estimation errors caused by the end effector layout, handling dynamics, and part geometry, and f_1, f_2, and f_3 are unknown functions to be identified.

The whole procedure for the dexterous model parameter estimation includes the following key steps:

1 *End effector layout selection*. A total number of *M* end effector layouts are selected for conducting the FEA simulation. The selection of the end effector positions depends on the part deformation modes of interest. For example, for a rectangular blank held in static condition, if end effectors are placed near the center of the part, its deformation mode is a convex curve as shown in Fig. 9 of Section 4.1.1. When end effectors are placed near the edge of the part, its deformation mode is a concave curve as shown in Fig. 11 of Section 4.1.1. Based on the number of modes of interest, one can select the positions to place the end effectors. The number of end effector layouts (equal to *M*) depends on the required estimation for accuracy and robustness. More accurate and robust estimation requires the FEA simulation to be conducted for a larger number of end effector layouts (see Section 3.2 for details).

2 *FEA simulation*. At each of the *M* end effector layouts, *m* FEA simulations are conducted. The number of simulations (equal to *m*) depends on the number of intended values for each variable to be estimated. The number of levels should be selected such as to span the real cup parameter range. More details are presented in Section 3.1.

3 *Experiments*. Experiments are conducted to test for part deformation at each of the *M* end effector layouts.

4 *Data processing*. The dexterous model parameters are estimated by developing an algorithm based on the simulation data and the experimental results. Details are presented in Section 3.2.

3.1 Part Deformation Simulation. The purpose of the FEA simulation is to investigate part deformation behavior under given key parameters of the dexterous model. One important finding in conducting this research is that sheet metal blanks usually have internal stress due to coiling or decoiling processing, and therefore, show some initial curvature in the natural status. When a blank is held by end effectors on its two different surfaces, the deformation contour of the blank is different. This phenomenon must be considered in the simulation since it significantly impacts the final blank deformation. The initial curvature is reflected in the FEA mesh of the handled blank.

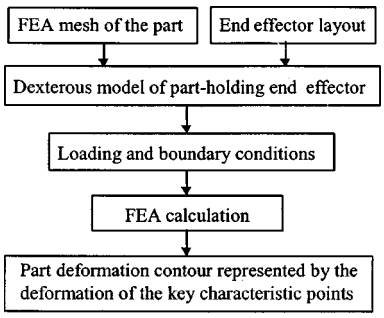

Fig. 6 Flowchart for the part deformation simulation

Figure 6 shows the flowchart of the part deformation simulation procedure. First, the FEA geometry mesh of the part is established including its initial curvature. Then, at a given end effector layout, the dexterous end effector model is generated by the method presented in Section 2. Next, loading and boundary conditions are applied to the whole model, and part deformation is calculated. In the output, part deformations at predetermined key characteristic points are recorded. The key characteristic points are selected by a product designer to reflect the critical discrete points used to determine an acceptable deformation contour of the whole part.[1]

Figure 6 shows the procedure for one simulation cycle. At each end effector layout, a total of *m* simulations are conducted. A design of simulations (DOS) approach is used to organize the conducted simulations. The purpose of DOS is to understand the overall part deformation behavior quantitatively. In addition, it is one part of the parameter estimation approach (see Section 3.2). The design variables used during simulations are the dexterous model stiffness, diameter, and height. The number of levels for each variable is determined based on the practical experience following the general guidelines used in the Design of Experiments (DOE) approaches [26].

3.2 Data Processing. After conducting the simulations, the deformations of the *M* sets of simulated key characteristic points are obtained. Each simulation set includes *m* simulations with different stiffness k_m, diameter d_m, and height h_m. Data processing includes the following steps:

1 For each one of the *m* simulation results at each of the *M* end effector layouts, deformation of the key characteristic point is expressed as a polynomial equation by fitting all the deformation data:

$$Y\_fit = \sum_{j=0}^{n} a_j x^j = a_n x^n + a_{n-1} x^{n-1} + \cdots + a_1 x + a_0 \tag{2}$$

where a_j is the coefficient of the polynomial function, x represents the coordinate along the line passing key characteristic points, and n is the order of the polynomial equations.

2 The relationship between each coefficient a_j (coefficient for x^j) and the variables k_m, d_m, h_m, (represented by k, d, and h respectively, in the following equations), is derived by the least square curve fitting for all the above *m* polynomial equations.

$$a_j = \sum_{i=1}^{l} c_i k^i + \sum_{j=1}^{p} s_j d^j + \sum_{r=1}^{q} w_r h^r + a_{j0} \tag{3}$$

[1]The key characteristic points are used to define the most important and most sensitive features of the product (points on the product where excess variation will most significantly affect product quality and performance), and of the process (points which are used to control the manufacturing process in order to maintain the product quality, for example, fixture locators). See [22–25] for more details.

where c_i, s_j and w_r are coefficients for polynomial equation of stiffness k, diameter d, and height h, respectively, l, p and q are the order of the polynomial equation of k, d and h respectively. a_{j0} is the residual constant after the fitting.

3 By substituting a_j in Eq. (2) using Eq. (3), Y_fit is expressed by a function of k, d and h.

$$Y\_fit = f(k,d,h) \tag{4}$$

4 The experimental data are used to estimate the values of k, d, and h. The values of k, d, and h should minimize the difference between Y_fit and the experimental deformation curve for all the M cup holding layouts. The problem is then transformed to the following optimization problem:

$$\min \sum_{j=1}^{M} \left\{ \sum_{i=1}^{N} [Y\_fit(x_i) - Y\_test(x_i)]^2 \right\}_j \quad with: k \geqslant 0, d \geqslant 0, h \geqslant 0 \tag{5}$$

where x_i represents the key characteristic point, and N is the number of key characteristic points.

5 The spring stiffness k, diameter d and height h are obtained by solving the above optimization problem.

4 Validation of the Developed Methodology

4.1. Case Study. A case study is performed to illustrate the procedures of the previously presented methodology and to verify its validity. The sample part is a steel sheet metal blank with dimensions of 924 mm by 260 mm by 0.6 mm (Fig. 7).

The elastic modulus E is 2.07×10^5 MPa and Poisson's ratio is $\nu = 0.3$. The center of the part is set as the origin of the coordinate system. The end effector locations vary along the line $y = \pm 70$ mm. The initial shape of the part is convex with the center point 30 mm above the edge points (Fig. 8b).

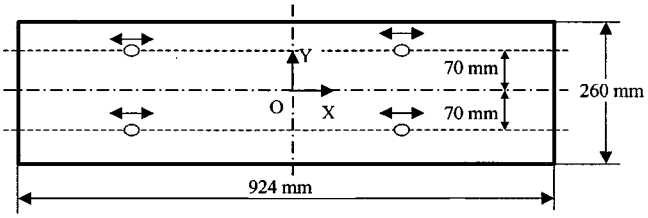

Fig. 7 The sample part and the coordinate system

4.1.1 FEA Simulation. In the FEA analysis, HYPERMESH was used for the geometry meshing and ABAQUS was used for the analysis and the post-processing. The part was modeled using shell elements with mesh size of 10 mm by 10 mm. The geometry mesh of the sample part is shown in Fig. 8. In Fig. 8, the points 2319, 2274, 2293, 2425, 2419, 2410, 1749, 1739, 1698, 1884, 1870, 261, 1183, 1162, 1319, 1310, 1275, 643, 634, 616, 770, 720, and 734 are selected as key characteristic points whose deformation represent the deformation contour of the sample part.

A DOS is performed to determine all parameters of the dexterous model. The dexterous model used in this case study is a 4-spring model constructed as shown in Fig. 4. The height in the spring model has relatively less impact on the holding-induced part deformation. Therefore, as a starting point, we will take the height of the physical cup as the height in the dexterous model. Following the acceptable variable ranges in real industrial applications, the value for each variable at each selected level is set as follows:

1 spring stiffness (N/mm): 0.5; 1; 2; 5; 10; 20; 50; and 100
2 dexterous model diameter (mm): $20\sqrt{2}$; $40\sqrt{2}$; and $100\sqrt{2}$
3 dexterous model height (mm): 10

Spring stiffness is the most critical parameter in the development of the dexterous model. The stiffness value 0.5 N/mm stands for the softest spring, and 50 N/mm stands for the hardest spring used in industrial application to handle parts similar to the presented case. We have also added stiffness of $k = 100$ N/mm to test the dexterous modeling limitations for cups which behave approximately as rigid points in considered cases. The simulated deformation is more sensitive to the smaller values of stiffness than the larger values. Thus, more stiffness values are selected at the lower end of the stiffness range (close to 0.5 N/mm). A general guideline for selection of variable levels in design of experiments is presented in Wu and Hamada [26].

The end effector holding positions are selected at $x = \pm 200$ mm and $x = \pm 400$ mm to represent two different deformation modes of the part. Later, we will use $x = 200$ mm and $x = 400$ mm to indicate these two layouts. The three aforementioned dexterous model diameters $20\sqrt{2}$, $40\sqrt{2}$, and $100\sqrt{2}$ will be represented in further description by $d = 10$ mm, $d = 20$ mm, and $d = 50$ mm respectively. This representation links the dexterous model diameters to the multiplication of the mesh size (10 mm in

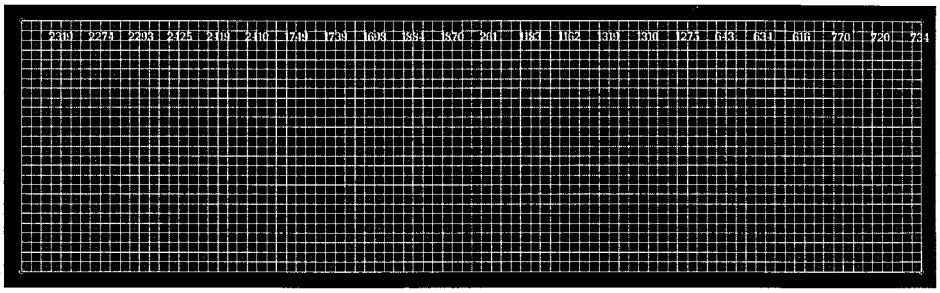

(a) Top view

(b) Front view

Fig. 8 Geometry mesh and target points for the sample part

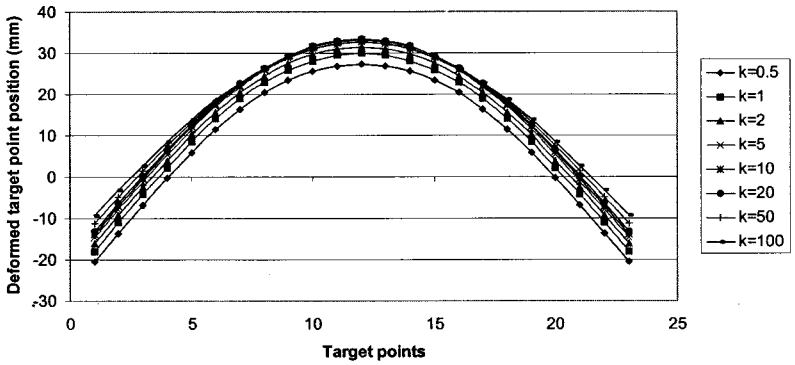

Fig. 9 Simulation for $x=200$ mm and $d=20$ mm

this case) and does not represent exact diameter of the models; however, this notation helps to visually locate the model. Following the procedures presented in Section 3, we have: $M=2$, and $m=24$ (8*3*1). Figures 9 through 11 show some selected examples of the simulation results.

We can see that end effector holding positions ($x=200$ and $x=400$), spring stiffness ($k=0.5$; 1; 2; 5; 10; 20, 50 and 100) and model diameter ($d=20$ and 50) have an impact on part deformation. With the same stiffness and dexterous model cup diameter, different holding positions cause dramatically different part deformation contours (compare Figs. 9 and 11). The sensitivity of part deformation to the stiffness increases when holding positions are near the edge of the part (compare Fig. 9 and Fig. 11), or when the spring model diameter is larger (compare Fig. 9 and Fig. 10).

It should be also noted that for simulations of dexterous models with very large values of stiffness (k) FEM simulations may not converge due to some FEM-based numerical problems. For example, for the case when part is held at position $x=400$ mm, and with the largest stiffness equal to $k=100$ N/mm, FEA analysis conducted using ABAQUS diverges (thus, a total of 21 simulations were conducted). This does not affect the accuracy of the presented results (see Fig. 13), however, it allows for the assessment of limitations of the FEM-based dexterous model. It is suggested that for the end effectors with very large stiffness it would be more appropriate to use a rigid point end effector model as presented in Ceglarek et al. [1] instead of a dexterous model.

The computational cost depends on the number of simulations, variable values, and holding positions. For each simulation, it took from several seconds to 20 minutes of CPU time on a HP 9000/C110 workstation with 128 MB RAM. For example, when holding position is at $x=400$ mm, stiffness is $k=20$ N/mm and spring diameter is $d=20$ mm, the total CPU time is 334 seconds. Computational time increases for larger values of stiffness and for holding position at $x=400$ mm.

4.1.2 Dexterous Model Parameter Estimation. In our study, the origin of the coordinate system is set at the center of the part

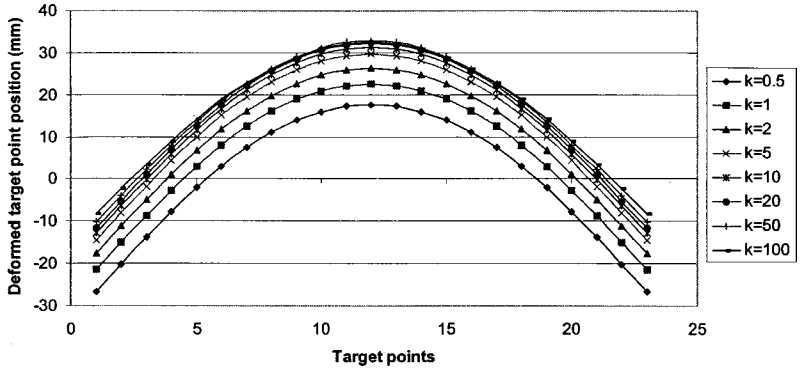

Fig. 10 Simulation for $x=200$ mm and $d=50$ mm

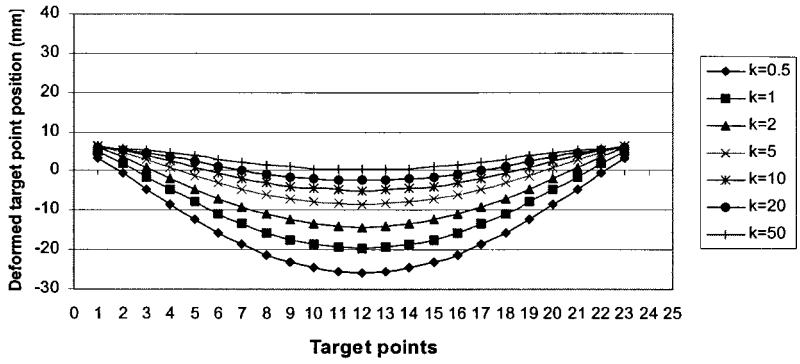

Fig. 11 Simulation for $x=400$ mm and $d=20$ mm

geometry, thus, resulting in part deformation to be symmetric and therefore, the polynomial equation for each individual simulation curve is an even function. Curve fitting and model order selection procedure was based on the comparison of residual errors and resulted in selection of the 4th order (residual error is on the same level for 4th and 6th order models), i.e., $n=4$. The generic equation for the 4th order even polynomial function is:

$$Y\_fit = a_4 x^4 + a_2 x^2 + a_0 \tag{6}$$

The relationship between each polynomial coefficient and the stiffness k and diameter d (as presented in Eq. (3)) is found through curve fitting. The model fitting procedure conducted is determined by residual error and coefficient of determination (R^2) [27]. The principle is to select the lower order model satisfying residual error criterion and R^2. The linear model is adequate regarding the relation for holding position at 200 mm ($R^2=0.966$), and acceptable for holding position at 400 mm ($R^2=0.844$). The relations between part deformation and the stiffness k and cup diameter d is as follows:

For holding at $x=200$ mm,

$$\begin{aligned} a_4 &= -5.0\times10^{-7}k - 1.2\times10^{-6}d + 6.09\times10^{-1} \\ a_2 &= 5.0\times10^{-4}k + 9.0\times10^{-4}d - 4.84\times10^{-1} \\ a_0 &= 3.93\times10^{-2}k - 1.19\times10^{-1}d + 33.3 \end{aligned} \tag{7}$$

For holding position at $x=400$ mm,

$$\begin{aligned} a_4 &= 6.9\times10^{-6}k + 8.0\times10^{-7}d - 4.98\times10^{-4} \\ a_2 &= -9.2\times10^{-3}k - 1.4\times10^{-3}d + 2.94\times10^{-1} \\ a_0 &= 1.12k - 2.11\times10^{-2}d - 19.9 \end{aligned} \tag{8}$$

Therefore, we get

$$\begin{aligned} Y\_fit\_200 &= A_1 k + B_1 d + C_1 \\ Y\_fit\_400 &= A_2 k + B_2 d + C_2 \end{aligned} \tag{9}$$

where A_1, B_1, C_1, A_2, B_2, C_2 are functions of the target point position x.

The experiments were conducted using the experimental setup and equipment described in Section 4.2. The final fitting problem as described in Eq. (5), i.e. the optimization problem, is transformed to minimize:

$$\sum_{i=1}^{23} [Y\_fit\_200(x_i) - Y\_test\_200(x_i)]^2 + \sum_{i=1}^{23} [Y\_fit\_400(x_i) - Y\_test\_400(x_i)]^2$$

$$with: k \geqslant 0, \quad d \geqslant 0 \tag{10}$$

This is a quadratic constrained optimization problem with variables k and d. The following result is obtained by solving this problem: $k=1.13$ N/mm, $d=18.72$ mm.

4.2 Experimental Setup and Equipment. A test-bed for the experimental verification of the methodology was set up to investigate the sheet metal part deformation behavior under different holding layouts as shown in Fig. 12. The tested part, necessary equipment as well as data acquisition system are as follows:

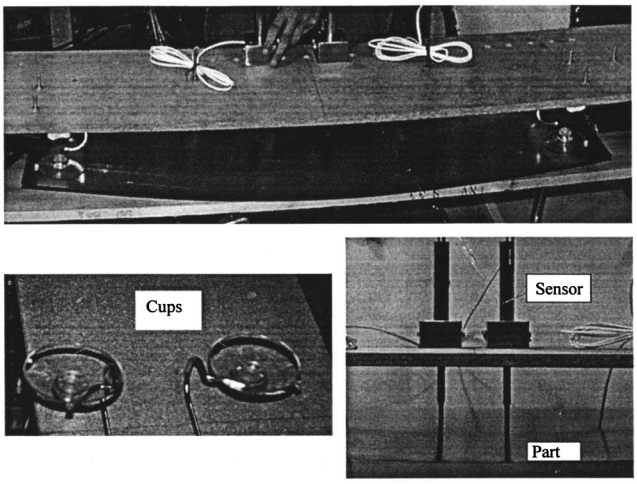

Fig. 12 Experimental setup and the test sensor

1 *Part*. The part dimension and material property are the same as that used in the simulation (section 4.1).

2 *Cups*. A set of cups is used in the experiment. The cups used are also shown in Fig. 12.

3 *Cup layouts*. The layouts at $x=200$ mm and $x=400$ mm are used for model parameter estimation. Different layouts are used to verify the validity of the developed modeling and parameter estimation methodology.

4 *Measurement device*. DC Fastar sensor is used to test part deformation. DC Fastar is a fast response transducer that measures linear displacement and absolute position. Its resolution is 0.001 percent of the full measurement range. The sensor used has a 4-inch measurement range, thus the resolution is 1 μm.

5 *Data acquisition system*. LABVIEW software is used to record the sensor signal in voltage reading.

4.3 Experimental Verification. To verify the validity of the proposed dexterous model parameter estimation algorithm, a new end effector layout at $x=250$ mm is chosen to conduct both the simulation and test. Since the model diameter cannot be randomly set for testing, we used $d=20$ mm to conduct all simulations. The value of $d=20$ mm is very close to the value of d presented in Section 4.1.2. The stiffness used is equal to $k=1.13$ N/mm.

The obtained results for both simulations and experimental testing are presented in Fig. 13. The maximum difference between

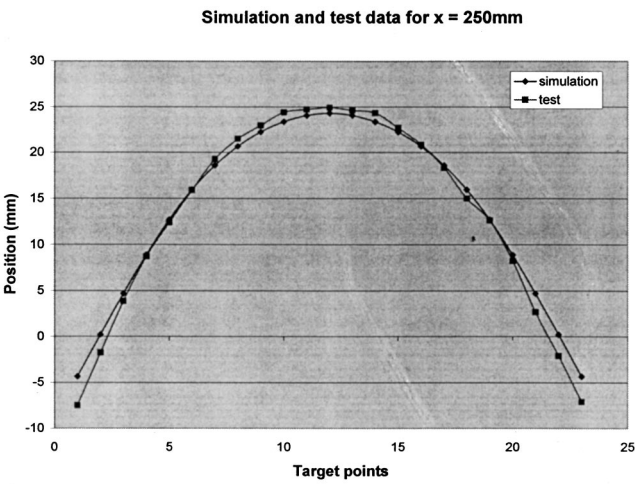

Fig. 13 Comparison of the simulation data with the experiment data

simulated and tested part deformations is 3.15 mm. The obtained results satisfy industrial requirements for part handling position accuracy (smaller than 6 mm).

Remarks: In the presented case, two holding layouts used for dexterous model estimation were sufficient to obtain the model, which is valid for various part holding layouts within presented application domain. It can also be concluded that parameter estimation of dexterous model by using a larger number of part holding layouts will allow for higher accuracy of model and expand validity of the model for larger domain of different part holding layouts. However, in industrial practice, one would like to use as small a number of layout as possible in the model parameter estimation procedure as long as the accuracy satisfies the requirements in the application domain.

4.4 Comparison with the Rigid Point End Effector Model. In order to demonstrate the advantages of the proposed dexterous model over the rigid model proposed by Ceglarek et al. [1], we conducted simulations of four different rigid point models and compared them with experimental testing of handling sheet metal part held by 4 vacuum cups. The four different rigid point models are generated by applying the following varying boundary conditions: *Model (1):* all the *x*, *y*, and *z* translational degrees of freedom (DOF) for all four end effectors are constrained; *Model (2):* the four end effectors (denoted by E_i, $i=1, 4$) are constrained as follows: E_1: all *x*, *y*, and *z* DOFs are constrained, E_2: *x* and *z* DOFs are constrained; E_3: *y* and *z* DOFs are constrained, E_4: *z* DOF is constrained; *Model (3):* the four end effectors are constrained as follows: E_1: all translational and rotational DOFs are constrained, E_2: *x*, *z* and all rotational DOFs are constrained; E_3: *y*, *z* and all rotational DOFs are constrained, E_4: *z* and all rotational DOFs are constrained, and *Model (4):* all the translational and rotational degrees of freedom are constrained. Model (2) simulates the deformation when the material flow is allowed between the end effectors, Model (3) is similar to Model (2), but it does not allow the rotational DOFs at the end effector locations. Simulations were conducted for two end effector layouts: at $x=200$ mm and at $x=400$ mm.

The simulation results for all four rigid point models and the test data for two part holding layouts are presented in Fig. 14 and Fig. 15.[2] It can be seen from Fig. 14 that when a holding position is at $x=200$ mm, only Model (2) can predict part deformation to the accepted tolerance limit of 6 mm. The accuracy of the other models exceed required tolerance limit. On the other hand, it can be seen from Fig. 15 that when a holding position is at $x=400$ mm, none of the four models can predict the deformation within the accepted tolerance limit. Moreover, models (1), (3) and (4) do not predict correct mode of part deformation. The presented results suggest that no rigid point models can predict part deformation with sufficient accuracy simultaneously for various part holding layouts required for a given application of handling parts using vacuum cups. It can be concluded that for compliant sheet metal parts, handled by material handling system with vacuum cups, a dexterous model is more appropriate. The rigid point models can be very effective for sheet metal parts handled by grippers, shovels or very rigid vacuum cups.

[2]It needs to be noticed that the curve of model (1) is overlapped with the curves of modesl (3) and (4) and cannot be seen in Fig. 14. The maximum distance between the two curves is smaller than 0.35 mm. In a similar way, the curve of model (1) is overlapped with the curve of model (4) and cannot be easily seen in Fig. 15. The maximum distance between the two curves is smaller than 0.12 mm.

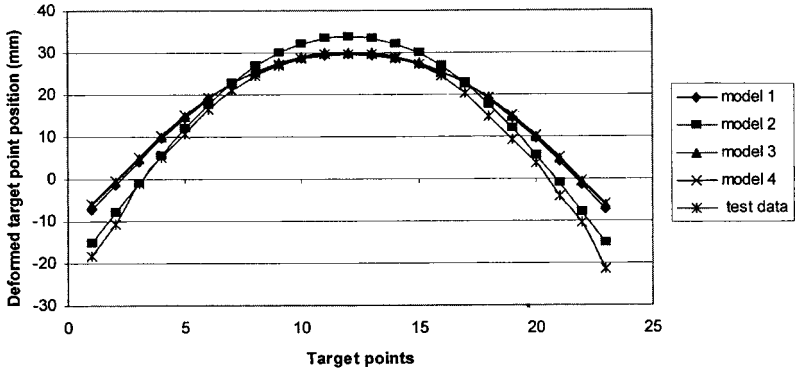

Fig. 14 Rigid point models comparison for holding layout position at 200 mm

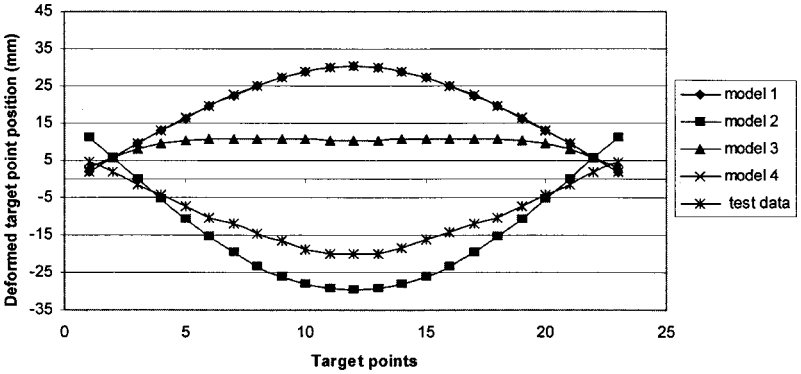

Fig. 15 Rigid point model comparison for holding layout position at 400 mm

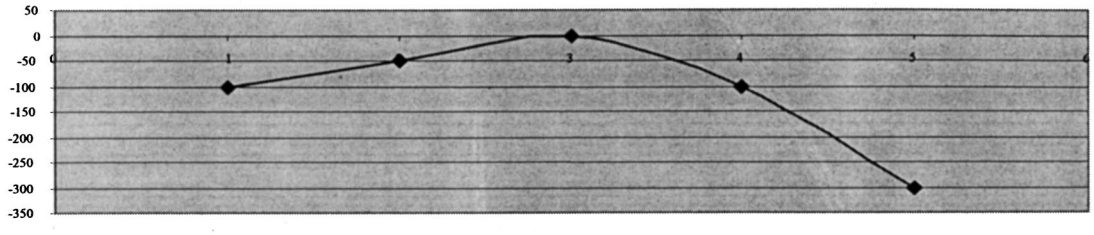

Fig. 16 Desired part deformation contour

4.5 Comparison of Optimal End Effector Locations. One of the most important applications of part deformation prediction is for the end effector location optimization. Ceglarek et al. [1] have presented an end effector location optimization technique based on a rigid end effector model. We applied this technique to a sheet metal blank using both the rigid model and a dexterous spring model. We selected the most appropriate case for the rigid point model to better understand its impact on the layout optimization. The objective function of the optimization is to minimize part deformation from a given die contour [1]. This objective function is used for handling sheet metal blanks before the first stamping operation and is formulated based on the premise that when part deformation shape is the same as the die contour, the nesting error is minimized and the stamped part has minimum dimensional variation.

The investigation is based on a sheet metal plate with a size of 960 mm by 260 mm by 1 mm. The die contour is approximated by the curve shown in Fig. 16. Five critical points on the sheet metal plate were selected to represent the entire deformation of the part and are also shown in Fig. 16. The objective function used for the optimization is to minimize the standard deviation of part deformation from the die contour as measured at five selected critical points.

The optimization results are listed in Table 2. The optimal end effector locations are schematically shown in Fig. 17. It can be seen that with the developed dexterous spring model, the resultant optimal end effector locations are different from those when using a rigid point model even for the case of using the most appropriate rigid point model. Thus, it is also suggested when to use the dexterous model in optimizing handling layout for part transfer using vacuum cups.

Table 2 Optimization results

	Objective function	Optimal locations
Rigid point model	43.8mm	(-292.1, -70.0), (-292.5, 69.0), (223.7, -76.8), (223.8, 77.1)
Dexterous model	42.2mm	(-269.6, -56.4), (-268.8, 56.2), (231.8, -64.7), (238.6, 60.7)

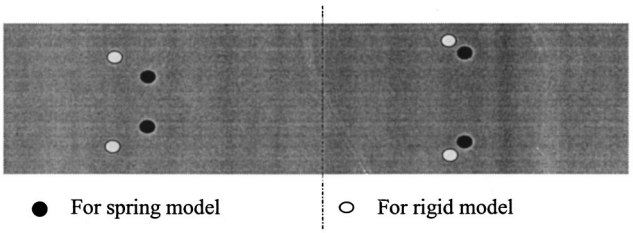

Fig. 17 The optimal end effector locations

5 Conclusions

Material handling of compliant sheet metal is a critical yet underresearched area in sheet metal stamping. One of the most challenging issues is the elastic part deformation during the handling process, which significantly impacts both part dimensional quality and the production rate. The elastic part deformation increases the possibility of part nesting error in dies, part distortion during contact with die as well as potential part-system interferences. It is very critical during material handling to control elastic deformation of parts. This paper advances previously developed material handling end effector layout optimization methodology for rigid point end effectors [1] by developing a dexterous part-holding end effector model. This model overcomes the shortcomings of the rigid point part-holding end effector model by predicting part deformation more accurately for various modes of deformation and for a domain of part-holding end effector location. This is especially important for handling systems with vacuum cups type of end effectors widely used for handling large sheet metal parts. In addition, it generates more accurate optimal end effector locations, which can be used to improve the material handling tooling design. The presented results showed that no rigid point models can predict part deformation with sufficient accuracy simultaneously for various part holding layouts required for handling parts using vacuum cups. It can be concluded that the dexterous model is more appropriate for compliant sheet metal parts handled by material handling systems with vacuum cups. The rigid point models can be effective for sheet metal parts handled by grippers, shovels or very rigid vacuum cups.

The dexterous end effector model design method and an algorithm for estimation of model parameters are developed. The algorithm combines data from design of computer simulations and from the set of experiments by integrating finite element analysis and a statistical data processing technique. Experimental studies are conducted to verify the developed dexterous cup model and the model parameter estimation algorithm. The parameter estimation algorithm provides accurate estimation of model parameters valid for a selected domain of part holding layouts based on experiments with only two pre-selected layouts. The developed model and methodology provides an analytical tool for product and process designers to be used for accurate prediction of part deformation during handling which further leads to minimization of part deformation and improvement of part dimensional quality and rate of production.

Acknowledgment

This research is partially supported by the Atlas Automation Inc., DaimlerChrysler, General Motors, and State of Wisconsin IEDR Program. The authors would like to acknowledge Mr. Jian Yao for his constructive suggestions and help with the experiments conducted in the research.

References

[1] Ceglarek, D., Li, H. F., and Tang, Y., 2001, ''Modeling and Optimization of Fixture for Handling Compliant Sheet Metal Parts,'' ASME J. Manuf. Sci. Eng., **123/3**, pp. 473–480.

[2] Li, D., Ceglarek, D., and Shi, J. 1993, ''Sliding Door Process Variation Study,'' *Technical Report for Chrysler Corp.*, The University of Michigan, Ann Arbor.

[3] Wu, X., Shi, J., and Hu, S., 1996, ''On-Site Measurement and Process Monitoring for Stamping Variation Reduction,'' *Technical Report, the 2mm Program, NIST-Advanced Technology Program*, pp. 61–80.

[4] Hockenberger, M., and DeMeter, E., 1995, ''The Effect of Machining Fixture Design Parameters on Workpiece Displacement,'' Manufacturing Review, **8/1**, pp. 22–33.

[5] Asada, H., and By, A., 1985, ''Kinematic Analysis of Workpart Fixturing for Flexible Assembly with Automatically Reconfigurable Fixtures,'' IEEE Journal of Robotics and Automation, **RA-1/2**, pp. 86–94.

[6] Chou, Y-C., Chandru, V., and Barash, M. M., 1989, ''A Mathematical Approach to Automatic Configuration of Machining Fixtures: Analysis and Synthesis,'' ASME J. Ind., **111**, pp. 299–306.

[7] Salisbury, J. K., and Roth, B., 1983, ''Kinematic and Force Analysis of Articulated Mechanical Hands,'' ASME J. Mech., Transm., Autom. Des., **105**, pp. 35–41.

[8] Nguyen, V., 1988, ''Constructing Force-closure Grasps,'' Int. J. Robot. Res., **7/3**, pp. 3–16.

[9] DeMeter, E. C., 1994, ''Restraint Analysis of Fixtures which Rely on Surface Contact,'' ASME J. Eng. Ind., **116/2**, pp. 207–215.

[10] Menassa, R., and DeVries, W., 1989, ''Locating Point Synthesis in Fixture Design,'' CIRP Ann., **38/1**, pp. 165–169.

[11] Menassa, R., and DeVries, W., 1991, ''Optimization Methods Applied to Selecting Support Positions in Fixturing Design,'' ASME J. Eng. Ind., **113**, pp. 412–418.

[12] DeMeter, E. C., 1995, ''Min-Max Load Model for Optimizing Machining Fixture Performance,'' ASME J. Eng. Ind., **117**, pp. 186–193.

[13] Lee, J. D., and Haynes, L. S., 1987, ''Finite Element Analysis of Flexible Fixturing Systems,'' ASME J. Eng. Ind., **109**, pp. 134–139.

[14] Youcef-Toumi, K., Liu, W., and Asada, H., 1988, ''Computer-Aided Analysis of Reconfigurable Fixtures and Sheet Metal Parts for Robotics Drilling,'' Rob. Comput.-Integr. Manufact., **4(3-4)**, pp. 387–394.

[15] Cai, W., Hu, S., and Yuan, J., 1996, ''Deformable Sheet Metal Fixturing: Principles, Algorithms, and Simulations,'' ASME J. Manuf. Sci. Eng., **118**, pp. 318–324.

[16] DeMeter, E. C., 1998, ''Fast Support Layout Optimization,'' Int. J. Mach. Tools Manuf., **38**, pp. 1221–1239.

[17] Li, B., and Melkote, S. N., 1999, ''Improved Workpiece Location Accuracy Through Fixture Layout Optimization,'' Int. J. Mach. Tools Manuf., **39/6**, pp. 871–883.

[18] Oden, J. T., and Pires, E. B., 1983, ''Nonlocal and Nonlinear Friction Laws and Variational Principles for Contact Problems in Elasticity,'' ASME J. Appl. Mech., **50**, pp. 67–76.

[19] Sinha, P. R., and Abel, J. M., 1992, ''A Contact Stress Model for Multi-Fingered Grasps of Rough Objects,'' IEEE Trans. Rob. Autom., **8/1**, pp. 7–22.

[20] Yeh, J. H., and Liou, F. W., 1999, ''Contact Condition Modeling for Machining Fixture Setup Processes,'' Int. J. Mach. Tools Manuf., **39/5**, pp. 787–803.

[21] Lin, L. R., and Huang, H. P., 1998, ''NTU Hand: A New Design of Dexterous Hands,'' ASME J. Mech. Des., **120/2**, pp. 282–292.

[22] Ceglarek, D., Shi, J., and Wu, S. M., 1994, ''A Knowledge-based Diagnosis Approach for the Launch of the Auto-body Assembly Process,'' ASME J. Eng. Ind., **116/4**, pp. 491–499.

[23] Ceglarek, D., and Shi, J., 1995, ''Dimensional Variation Reduction for Automotive Body Assembly,'' Manufacturing Review, **8/2**, pp. 139–154.

[24] Thornton, A. C., 1999, ''A Mathematical Framework for the Key Characteristic Process,'' Res. Eng. Des. **11** (3), pp. 145–157.

[25] Ceglarek, D., and Shi, J., 1998, ''Design Evaluation of Sheet Metal Joints for Dimensional Integrity,'' ASME J. Manuf. Sci. Eng., **120/2**, pp. 452–460.

[26] Wu, C. F. J., and Hamada, M., 2000, *Experiments: Planning, Analysis, and Parameter Design Optimization*, John Wiley and Sons.

[27] Dielman, T., 2001, *Applied Regression Analysis*, Duxbury Thomson Learning.